Article:
Mahon, CS, Wildsmith, GC, Haksar, D et al. (5 more authors) (2019) A 'catch-and-release' receptor for the cholera toxin. Faraday Discussions, 219. pp. 112-127. ISSN 1359-6640

https://doi.org/10.1039/c9fd00017h

A 'catch-and-release' receptor for the cholera toxin

Clare S. Mahon,*[a,b] Gemma C. Wildsmith,[a] Diksha Haksar,[c] Eyleen de Poel,[d] Jeffrey M. Beekman,[d] Roland J. Pieters,[c] Michael E. Webb[a] and W. Bruce Turnbull,*[a,b]

Stimuli-responsive receptors for the recognition unit of the cholera toxin (CTB) have been prepared by attaching multiple copies of its natural carbohydrate ligand, the GM1 oligosaccharide, to a thermoresponsive polymer scaffold. Below their lower critical solution temperature (LCST), polymers complex CTB with nanomolar affinity. When heated above their LCST, polymers undergo a reversible coil to globule transition which renders a proportion of the carbohydrate recognition motifs inaccessible to CTB. This thermally-modulated decrease in the avidity of the material for the protein has been used to reversibly capture CTB from solution, enabling its convenient isolation from a complex mixture.

Introduction

Interactions between proteins and other biological macromolecules or surfaces are crucial to the mediation of many physiological processes in healthy and diseased states,[1] and the development of synthetic materials which can perturb such interactions presents exciting opportunities for the production of new therapeutics and diagnostics.[2, 3] Proteins often associate with their binding partners across large interface areas through multivalency,[4] harnessing the effects of multiple weak interactions to produce strong adhesive forces. The construction of receptors or inhibitors using polymer-based systems allows for convenient access to the large molecular architectures required to bridge recognition sites on the surfaces of proteins, eliminating the need for the demanding synthesis of complex architectures such as dendrimers.[5] The choice of a synthetic polymer scaffold for the construction of receptors also enables the inclusion of secondary functionality, such as compositional adaptivity,[6, 7] or the ability to respond to environmental stimuli such as temperature[8] or pH,[9] to produce an adaptive material.

The inclusion of thermoresponsive functionality within macromolecular receptors for proteins has yielded highly-functional materials which allow for tunable recognition of their targets. Gibson and coworkers[10] have produced temperature-responsive nanoparticle-based receptors by immobilising polymers with α-terminal aminogalactosyl units onto gold nanoparticles, along with a thermoresponsive polymer designed to act as a 'gate.' Below the lower critical solution temperature (LCST) of the 'gate' polymer, its steric bulk prevents the carbohydrate motifs from accessing the binding sites of soybean agglutinin (SBA), a complementary lectin. Heating the material induces collapse of the of the 'gate' polymer, exposing carbohydrate units on the surface of the nanoparticles which are then able to complex with SBA. A similar strategy has been used to control the surface presentation of receptor targeting ligands on polymer-decorated nanoparticles, and thereby control their endocytosis. Alexander and coworkers[11] have decorated gold nanoparticles with transferritin, an iron transporting protein, along with a 'shielding' thermoresponsive polymer. Below the LSCT of the polymer, nanoparticles display poor cellular uptake. An increase in temperature can be used to trigger collapse of the 'shielding' polymer, exposing the transferrin ligands and inducing cellular uptake. An impressive 'catch-and-release' system for a protein has been developed by Shea and coworkers,[12] where multicomponent polymer nanoparticles were demonstrated only to complex lysozyme above their LCST, enabling their binding to the protein and subsequent release upon cooling. Surface-bound polymer brushes have also been employed for the selective adsorption of proteins, by tuning the ionic strength of the surrounding medium to modulate electrostatic interactions between proteins and surfaces.[13]

Here, we have constructed a high-affinity multivalent receptor for a bacterial protein on a thermally responsive polymer scaffold, and demonstrated that an increase in temperature above the LCST of the polymer may modulate this recognition – a feature we have used to enable the isolation of a single protein from a complex mixture.

Our thermoresponsive receptor binds to the carbohydrate recognition domain of the cholera toxin,[14] a protein produced by *Vibrio cholerae* in the human intestine which is responsible for the acute diarrhoea associated with cholera. The cholera toxin is comprised of a single toxic A subunit and non-toxic B_5 pentamer of identical units (CTB), each possessing a recognition site for the GM1 ganglioside (GM1), which is displayed on intestinal epithelial surfaces. The pentasaccharide unit of the ganglioside, the GM1 oligosaccharide (GM1os), has been demonstrated by isothermal titration calorimetry to display a remarkably high affinity for CTB, with a reported K_d of ~40 nM.[15] Already, the incorporation of multiple copies of GM1os on macromolecular scaffolds[16, 17] such as dendrimers,[18] synthetic polymers[19] or proteins[20] has been shown to greatly enhance the inhibitory potency of recognition units, making CTB a particularly attractive target for the development of 'smart' multivalent receptors and inhibitors.

Results and discussion

Synthesis of thermoresponsive receptor

We chose to construct our receptor on a poly(*N*-isopropylacrylamide) (poly(NIPAm)) scaffold, a class of polymer well known for its ability to reversibly desolvate upon increases in solution temperature.[21] NIPAm was copolymerised with *tert*-butyl 2-

methacryloylhydrazine-1-carboxylate (M1) (Scheme 1), which was prepared via hydrazinolysis of methacrylic anhydride,[22] and subsequent BOC-protection of hydrazide units. RAFT polymerisation afforded a copolymer with a degree of polymerisation of approximately 99, displaying approximately 21 protected acylhydrazide functionalities as estimated using ^{1}H NMR spectroscopy. Subsequent deprotection of P1 yielded the multiply acylhydrazide-functionalised P2, which enabled the direct functionalisation of polymers with reducing sugars through the formation of

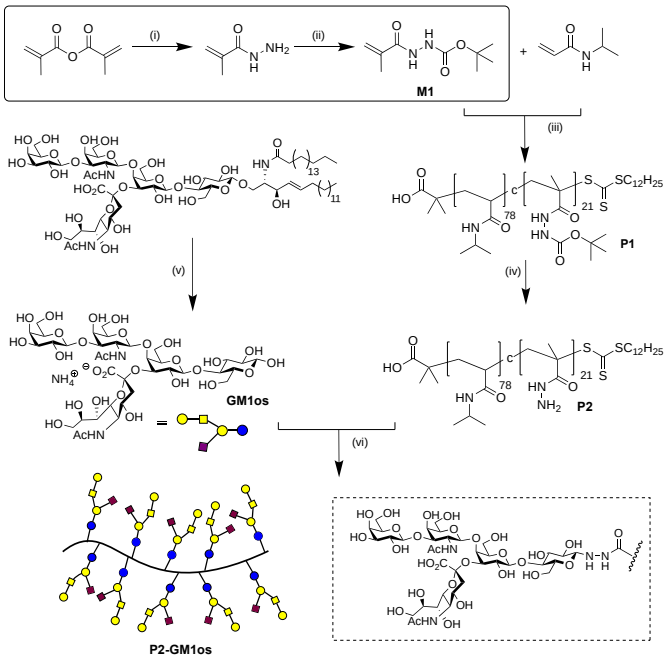

Scheme 1 Preparation of **P2-GM1os**. (i) $N_2H_4.H_2O$, $CHCl_3$, rt, 1 h. (ii) Di-*tert*-butyl dicarbonate, THF, rt, 24 h. (iii) *S*-Dodecyl-*S*′-(α,α′-dimethyl-α′′-acetic acid)trithiocarbonate, 2,2′-azobis(2-methylpropionitrile), DMSO, 70 °C, 18 h. (iv) 50 % v/v CH_3COOH, CH_2Cl_2, rt, 1 h. (v) EGCaseII, 25 mM NH_4OAc, pH 5.0, 0.2 % v/v Triton X-100. (vi) 100 mM NH_4OAc, pH 4.5, rt, 18 h.

β-glycoside linkages (Scheme 1). This strategy has been used for the preparation of surface-immobilised carbohydrate microarrays,[23] and avoids potentially complex synthetic modifications of the oligosaccharide in addition to presenting a general route to the production of receptors for other carbohydrate binding proteins. The GM1 ganglioside was treated with a bacterial endoglycoceramidase (EGCaseII, *Rhodococcus sp. M-777*) to yield GM1os,[24, 25] which was combined with **P2** under mildly acidic conditions to yield a polymer functionalised with multiple copies of GM1os (**P2-GM1os).** ^{1}H NMR spectroscopic analysis (ESI Fig. S2) confirmed the oligosaccharide to be displayed on the polymer primarily as its β-glycoside. Dynamic light scattering (DLS) analysis (Fig. 2(c)) of **P2-GM1os** revealed a monomodal distribution with number average hydrodynamic diameter (D_h) of approximately 16 nm, a significant increase in hydrodynamic volume compared to **P2**, which displayed a D_h of approximately 5 nm.

Assessment of inhibitory potency of P2-GM1os for CTB

As other multivalent receptors for CTB have previously proven effective in inhibiting adhesion of the cholera toxin to GM1 functionalised surfaces, [26, 27] we decided to investigate this effect with our system. Initially, the inhibitory potency of **P2-GM1os** towards CTB was assessed using an enzyme-linked lectin assay (ELLA, Fig. 1),[20] where the ability of CTB to bind to surface-immobilised GM1 was assessed over a range of **P2-GM1os** concentrations (Table 1) at 25 °C. **P2-GM1os** demonstrated an IC_{50} value of 3.78 nM, a significant enhancement in inhibitory potency compared to GM1os (Table 1, 505 nM), demonstrating that **P2-GM1os** can effectively disrupt interactions between CTB and surfaces displaying GM1os. We next investigated the ability of **P2-GM1os** to prevent the entry of the cholera toxin to human cells, using an intestinal organoid assay.[28] In this assay, intestinal organoids are exposed to the cholera toxin over a range of inhibitor concentrations, and inhibition is monitored by assessing the ability of the cholera toxin to enter the cells and to induce fluid secretion leading to an increase in organoid surface area. **P2-GM1os** was found to be a potent inhibitor of cholera toxin induced swelling, with an IC_{50} value of 5.68 nM, demonstrating an impressive improvement in inhibitory

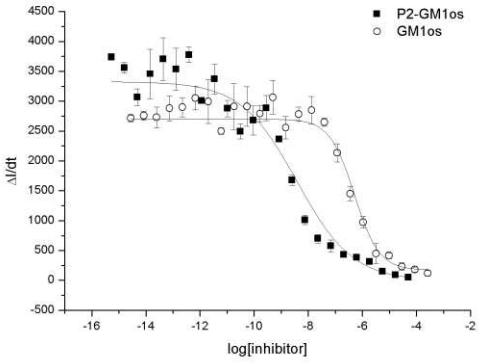

Fig. 1 Enzyme-linked lectin assay (ELLA) indicates the inhibitory potency of **P2-GM1os** compared to GM1os at 293 K. Error bars indicate the standard error of three measurements.

Table 1 Inhibitory potencies from enzyme-linked lectin assay (ELLA) and intestinal organoid assay. Curves were fitted using log[inhibitor] values, leading to the asymmetric distribution of fitting errors about the mean. These errors have therefore been omitted for simplicity. [a] Potency is expressed relative to monovalent GM1os in the corresponding assay.

Assay	Inhibitor	Valency	log[IC_{50}]	IC_{50} / nM	Relative potency (per GM1os)
ELLA	GM1os	1	-6.30 ± 0.08	505	1
ELLA	**P2-GM1os**	21	-8.42 ± 0.14	3.78	6.38
Intestinal organoid assay	GM1os	1	-5.06 ± 0.11	8700	1
Intestinal organoid assay	**P2-GM1os**	21	-8.30 ± 0.16	5.68	72.9

potency compared to GM1os (Table 1, 8.7 μM). These results demonstrate that the complexation of CTB by **P2-GM1os** can be harnessed to prevent the internalisation of the cholera toxin by intestinal cells. Synthetic multivalent inhibitors of cellular adhesion such as **P2-GM1os** may offer therapeutic potential for diseases caused by bacterial toxins, offering an attractive antibiotic-free route to the control of symptoms.[29]

Thermoresponsive behaviour

The thermoresponsive properties of **P2** and **P2-GM1os** were investigated by turbidimetry,[21] (Fig. 2(a),(b)) providing an estimate of the LCST of each polymer. **P2** was observed to undergo a sharp phase transition with a cloud point of 44 °C at 2.0 mg mL^{-1} in phosphate-buffered saline (137 mM NaCl, 2.7 mM KCl, 10 mM Na_2HPO_4, 1.8 mM KH_2PO_4, pH 7.4 - PBS). The analogous transition for **P2-GM1os** was observed to occur with a similar cloud point of 48 °C under the same conditions, but with the transition occurring over a broader temperature range, a feature we attribute to the numerous hydrogen bonding units incorporated onto **P2** by its functionalisation with GM1os. The cloud point determined for **P2-GM1os** by turbidimetry was in agreement with variable-temperature dynamic light scattering experiments conducted at 0.5 mg mL^{-1} in the same buffer (Fig. 2(d)), which showed the formation of large aggregates in solution around this temperature. We hypothesised that this triggered phase transition could be used to modulate the affinity of **P2-GM1os** for CTB, and decided to probe this hypothesis using isothermal titration calorimetry (ITC).

Isothermal titration calorimetry studies

Initially, recognition was investigated at 25 °C, below the LCST of the polymer, when chains adopt a hydrated coil conformation. Under these conditions, CTB was observed to recognise GM1os with a K_d of 37.9 nM (± 3.7 nM) (Fig. 3(a), Table 2). **P2-GM1os** also displayed nanomolar affinity for CTB, with an apparent K_d of 31.4 nM (± 4.1 nM) and a binding stoichiometry of 15 CTB subunits per polymer chain, demonstrating that multiple GM1os residues on each polymer can interact with CTB with a similar affinity to that observed for the monovalent interaction. The apparent lack of improvement in K_d, despite a significant enhancement in inhibitory potency, has been observed previously with other multivalent inhibitors of CTB.[20, 30] We next repeated these experiments at 60 °C, above the LCST of the polymer, when polymer chains are expected to exist in a collapsed, globular conformation. At this temperature CTB, which has been determined to be thermally stable at temperatures of up to 74 °C,[31] was shown to recognise GM1os with a K_d of 4.46 μM (± 0.43 μM) (Fig. 3(c), Table 2). This decrease in affinity at elevated temperature may be accounted for by the unfavourable entropic contribution to binding, and in particular the increase in flexibility of the loop around the carbohydrate recognition site of the protein.[32] Under these conditions, **P2- GM1os** binds CTB with an apparent K_d of 3.66 μM (± 0.81 μM) (Fig. 3(d), Table 2), similar to the monovalent interaction. Notably, however, the binding stoichiometry of the

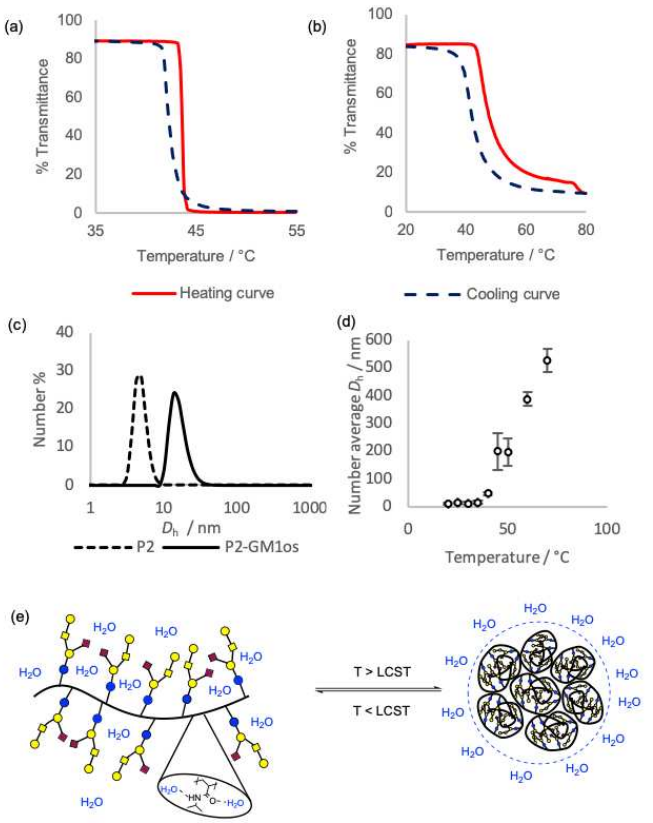

Fig. 2 Temperature-turbidity curves for **P2** (a) and **P2-GM1os** (b) at 2.0 mg mL-1 in PBS, pH 7.4 (137 mM NaCl, 2.7 mM KCl, 10 mM Na_2HPO_4, 1.8 mM KH_2PO_4). (c) Number average hydrodynamic diameters (D_h) for **P2** and **P2-GM1os** at 25 °C in PBS pH 7.4. (d) Number average D_h for **P2-GM1os** across the temperature range 20-80 °C. Error bars represent the standard distribution of at least five measurements. (e) The reversible desolvation of **P2-GM1os** at temperatures above its LCST.

interaction decreased to 9.9, suggesting fewer GM1os residues per polymer chain interact with CTB at elevated temperature. We propose that the thermally-triggered collapse of **P2-GM1os** renders a proportion of GM1os recognition units inaccessible to CTB on the interior of the globule, whilst the GM1os residues which remain on the surface still interact with CTB with a comparable affinity to the monovalent interaction. We

Table 2 Thermodynamic parameters for GM1os and **P2-GM1os** binding to CTB at 25 °C and at 60 °C. Titrations were performed in PBS at pH 7.4 (137 mM NaCl, 2.7 mM KCl, 10 mM Na_2HPO_4, 1.8 mM KH_2PO_4). *binding stoichiometry fixed during fitting.

Temp. / °C	Ligand	$K_{d\ (app)}$ / nM (σ)	ΔG / kcal mol^{-1} (σ)	ΔH / kcal mol^{-1} (σ)	ΔS / cal K^{-1} mol^{-1} (σ)	n (σ)
25	GM1os	37.9 (3.7)	-10.1 (1.0)	-20.5 (0.1)	-34.9 (4.9)	1.0 (0.004)
25	**P2-GM1os**	31.4 (4.1)	-10.2 (1.3)	-20.8 (0.2)	-35.5 (6.5)	14.8 (0.07)
60	GM1os	4460 (430)	-8.15 (0.8)	-30.1 (0.9)	-66.0 (8.9)	1.0*
60	**P2-GM1os**	3660 (810)	-8.29 (1.83)	-34.2 (4.3)	-77.7 (19.7)	9.9 (0.99)

hypothesised that this thermally-induced change in binding stoichiometry could be harnessed to modulate the overall avidity of the material for CTB. With this aim in mind, we

immobilised **P2-GM1os** onto a solid support, to investigate if the polymer could be used to facilitate 'catch-and-release' isolation of the protein.

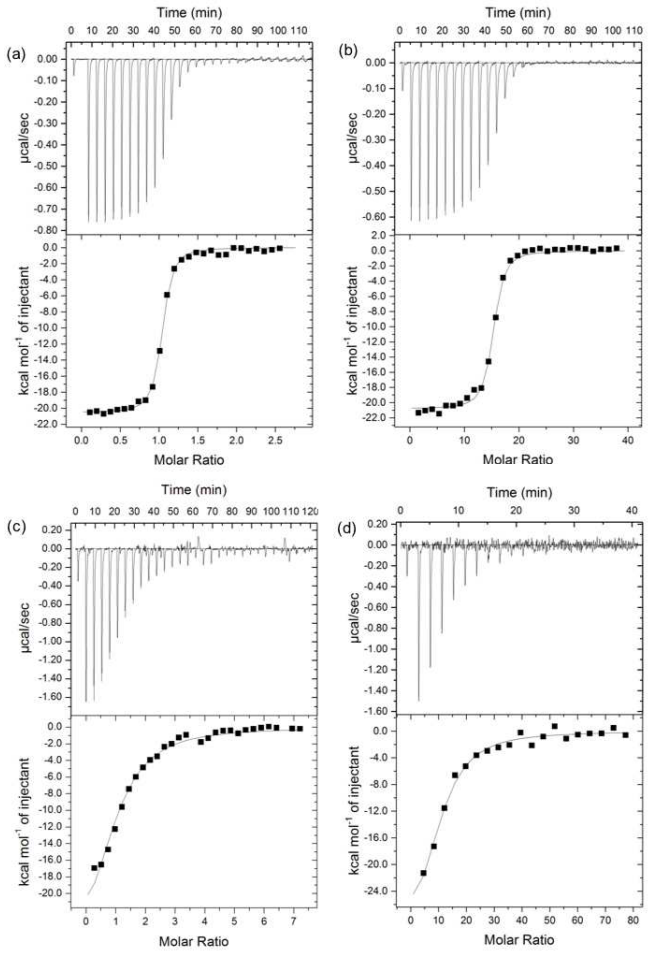

Fig. 2 Titrations of (a) 137 µM GM1os into 8.91 µM CTB at 25 °C; (b) 110 µM CTB into 0.5 µM P2-GM1os at 25 °C; (c) 376 µM GM1os into 9.32 µM CTB at 60 °C; and (d) 378 µM CTB into 1.0 µM P2-GM1os at 60 °C. CTB concentrations refer to the concentration of the B subunit.

Reversible complexation of CTB

P2-GM1os was conveniently immobilised onto a solid support in a in a one-pot procedure. The trithiocarbonate end groups of were first converted to thiols by aminolysis, and immediately

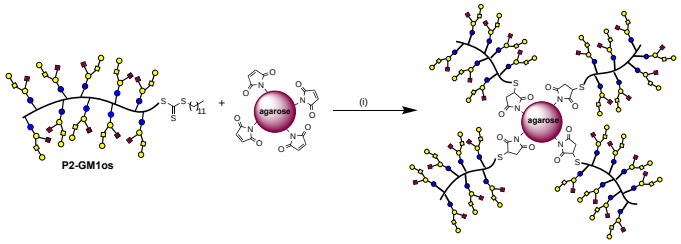

Scheme 2 Immobilisation of **P2-GM1os** onto maleimide-functionalised agarose beads. (i) hexylamine, Et_3N, DMSO.

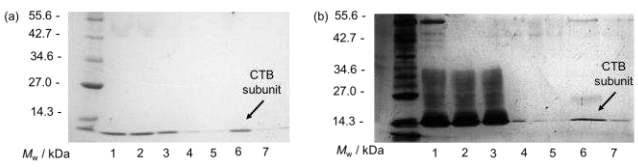

Fig. 4 The 'catch-and-release' behaviour of **P2-GM1os** functionalised beads applied to (a) a 10 µM solution of CTB in PBS pH 7.4; and (b) *Vibrio sp60* growth medium, as demonstrated by gel electrophoresis. In each case lane 1 contains the analyte; lane 2 beads after exposure to analyte; lane 3 the supernatant after analyte loading; lanes 4 and 5 contain the bead washes with PBS at room temperature; lane 6 contains the eluate obtained after treatment with PBS at 60 °C and lane 7 the beads after elution. Gels were stained using Coomassie blue (a); or silver stain (b).

subjected to thiol-ene coupling[33] with commercially available maleimide functionalised agarose beads (Scheme 2). Upon incubation with a 10 µM solution of CTB in PBS, beads were shown to complex with CTB using gel electrophoresis (Fig 4(a)). The CTB complexed with the beads was not eluted during washes with PBS at ambient temperature, but when incubated with the same buffer at 60 °C, above the determined LCST of **P2-GM1os**, CTB was successfully recovered from the beads. To determine if this 'catch-and-release'[12] behaviour could translate to the isolation of a single protein from a highly complex mixture, we attempted to isolate CTB from a solution of *Vibrio sp60* growth medium in which CTB is expressed, and exported from the cells to the surrounding medium. The cells were separated from the rest of the growth medium by centrifugation, and the supernatant incubated with **P2-GM1os** functionalised beads at room temperature. The beads were washed with PBS at room temperature to remove any weakly adhering material, before treatment with the same buffer at 60 °C triggered elution of CTB (Fig. 4(b)). This response demonstrates that the combined effects of high-affinity multivalent recognition and the stimuli-responsive nature of our polymer scaffold may be used to selectively isolate a single bacterial toxin from a complex biological medium.

Conclusions

In summary, we report a stimuli-responsive receptor which can complex CTB with nanomolar affinity, and release the protein on demand in response to a thermal stimulus. Our polymeric receptor has been shown to be effective in preventing the internalisation of the cholera toxin by intestinal cells, with inhibitory potency in the low nanomolar range. The temperature-mediated 'catch-and-release' behaviour has been used to isolate CTB from bacterial growth medium, a complex biological medium containing a multitude of other proteins. Current 'gold-standard' identification protocols for cholera[34] and other diarrheal diseases rely on bacterial culture, processes which require time and access to appropriate facilities. We anticipate that our system could contribute to the development of diagnostics for diseases such as cholera, by providing a route to conveniently isolate the toxin for identification.

Finally, our method presents a straightforward route to the synthesis of highly functional multivalent receptors for lectins, incorporating carbohydrate recognition motifs directly from reducing sugars. Our approach could be easily adapted to enable the production of receptors for the many other carbohydrate-binding proteins implicated in bacterial disease,[16] by judicious choice of carbohydrate recognition units.

Experimental

Materials and characterisation

All reagents were purchased from Sigma Aldrich, Alfa Aesar, Carbosynth or Fluorochem and used as received unless otherwise stated. *N*-isopropylacrylamide was recrystallised from hexane prior to use. Phosphate buffered saline (PBS) refers to a solution of 137 mM NaCl, 2.7 mM KCl, 10 mM Na_2HPO_4 and 1.8 mM KH_2PO_4 in MilliQ water. ^1H and ^{13}C NMR spectra were recorded on a Bruker Avance 500 spectrometer at 500 MHz and 125 MHz respectively, with the residual solvent signal as an internal standard. Mass spectra were collected using a Bruker MicroTOF instrument. Gel permeation chromatography (GPC) was conducted on a Varian ProStar instrument (Varian Inc.) equipped with a Varian 325 UV-Vis dual wavelength detector (254 nm), a Dawn Heleos II multi-angle laser light scattering detector (Wyatt Technology Corp.), a Viscotek 3580 differential RI detector, and a pair of PL gel 5 µm Mixed D 300 × 7.5 mm columns with guard column (Polymer Laboratories Inc.) in series. Near monodisperse methyl methacrylate standards (Agilent Technologies) were used for calibration. Data collection was performed with Galaxie software (Varian Inc.) and chromatograms analyzed with Cirrus software (Varian Inc.) and Astra software (Wyatt Technology Corp.). Turbidimetric analysis was performed on a Cary 100 UV-Vis spectrometer, with the absorbance of 2.0 mg mL^{-1} solutions monitored at 550 nm. Cloud points are reported as the mid-point of a fit to a standard dose-response curve in Origin 8. Dynamic light scattering (DLS) instrumentation consisted of a Malvern Zetasizer µV with a 633 nm HeNe laser module. Measurements were made at an angle of 173 ° (back scattering) and Malvern Zetasizer software was used to analyse the data. Solutions were filtered through a 0.22 µm PTFE filter prior to analysis. At each temperature point the solution was incubated for 30 min before measurements were made.

Methacryloyl hydrazide[22] (1)

Methacrylic anhydride (9.6 mL, 65 mmol) in $CHCl_3$ (50 mL) was added dropwise to hydrazine hydrate (13.2 mL, 27 mmol) at 0 °C. The mixture was left to stir at room temperature for 1 h, then the organic fraction was removed. The aqueous fraction was extracted with $CHCl_3$ (3 × 25 mL) and the combined organic extracts were dried over $MgSO_4$ and evaporated to dryness, yielding a while solid. The title product was recrystallised from 10:1 toluene : CH_2Cl_2 and isolated as colourless, needle-like crystals (2.50 g, 38%). ^1H NMR (500 MHz, $CDCl_3$): δ 1.95 (s, 3H, CH_3), 3.98 (s, 2H, NH_2), 5.35 (s, 1H, CH_2), 5.71 (s, 1H, CH_2), 7.39 (s, 1H, N*H*). ^{13}C NMR (125 MHz, $CDCl_3$): δ 18.5, 120.5, 138.2, 169.5. Melting point 83.0 – 86.5 °C (84 – 86 °C[22]). ESI-HRMS: calculated for $C_4O_2N_2H_9$ [M + H^+]: 101.0709; found 101.0019.

tert-Butyl 2-methacryloylhydrazine-1-carboxylate[35] (M1)

Di-*tert*-butyl dicarbonate (5.12 g, 24 mmol) in THF (50 mL) was added dropwise to **1** (2.38 g, 24 mmol) in THF (50 mL). The reaction mixture was left to stir at room temperature for 24 h before it was evaporated to dryness. The white solid obtained was dissolved in CH_2Cl_2 (100 mL) and washed with sat. $NaCl_{(aq)}$ (100 mL). The organic fraction was dried over $MgSO_4$ and evaporated to dryness, yielding a white solid. **M1** was recrystallised from 10:1 toluene : CH_2Cl_2 and isolated as white crystals (2.65 g, 55 %). ^1H NMR (500 MHz, $CDCl_3$): δ 1.47 (s, 9H, C(CH_3)$_3$), 1.98 (s, 3H, CH_3), 5.42 (s, 1H, CH_2), 5.81 (s, 1H, CH_2), 6.70 (s, 1H, NHN*H*COC(CH_3)$_3$), 7.89 (s, 1H, N*H*NHCO C(CH_3)$_3$). ^{13}C NMR (125 MHz, $CDCl_3$): δ 18.5, 28.3, 82.1, 83.62, 133.3, 155.7, 167.8. Melting point: 115.5 – 117.6 °C. ESI-HRMS: calculated for $C_9H_{16}N_2NaO_3$ [M + Na^+]: 223.1053; found 223.1057.

BOC-protected acylhydrazide copolymer P1

S-1-Dodecyl-*S'*-(α,α-dimethyl-α''-acetic acid)trithiocarbonate[36] (DDMAT) (20 mg, 5.5 × 10^{-5} mol, 1.0 eq.), *α,α'*-azoisobutyronitrile (AIBN) (1.8 mg, 1.1 × 10^{-5} mol, 0.2 eq.), *N*-isopropylacrylamide (NIPAm) (0.993 g, 8.78 mmol, 160 eq.) and **M1** (0.241 g, 1.20 mmol, 20 eq.) were combined in DMSO (3 mL) and degassed via three freeze-pump-thaw cycles. The vessel was backfilled with $N_{2(g)}$ and allowed to warm to room temperature, then placed in a preheated oil bath at 70 °C for 18 h. The polymerisation was quenched by rapid cooling in $N_{2(l)}$, followed by exposure to air. The solution was added dropwise to a large excess of ice-cold diethyl ether, yielding a yellow-white solid which was redissolved in THF and the precipitation repeated twice before drying under high vacuum. **P1** was isolated as a yellow-white solid (0.350 g). ^1H NMR (500 MHz, $CDCl_3$): δ 1.15 (br, NHCH(CH_3)$_3$), 1.48 (br, (COOC(CH_3)$_3$), 1.6 – 1.9 (br, (CH_2, CH_3), polymer backbone), 2 – 2.4 (br, (C*H*), polymer backbone, 3.04 (br, N*H*CHCH$_3$), 4.01 (br, NHC*H*CH$_3$), 6.0-7.0 (br, N*H*N*H*COOC(CH$_3$)$_3$).

Acylhydrazide copolymer P2

P1 (30 mg, 2.2 × 10^{-6} mol) was dissolved in CH_2Cl_2 (1 mL). Trifluoroacetic acid (1 mL) was added and the solution was left to stir at room temperature for 1 h. The solution was concentrated *in vacuo*, yielding a yellow glassy film which was redissolved in H_2O, dialysed against H_2O and lyophilised, yielding **P2** as a yellow-white solid (21 mg, 83% yield). ^1H NMR (500 MHz, $CDCl_3$): δ 1.13 (br, NHCH(CH_3)$_3$, polymer backbone), 1.6 – 1.9 (br, (CH_2, CH_3), polymer backbone), 2 – 2.4 (br, (C*H*), polymer backbone, 4.01 (br, NHC*H*CH$_3$).

GM1os functionalised copolymer P2-GM1os

GM1os (6.2 mg, 6.1 x 10^{-6} mol) and **P2** (3.0 mg, 2.6 × 10^{-6} mol) were combined in 100 mM NH_4OAc, pH 4.5, D_2O (500 µL). The solution was left to stir at room temperature for 24 h. The solution was then dialysed against H_2O and lyophilised, yielding the title product as a yellow-white solid (3.5 mg, 41% yield). ^1H NMR (500 MHz, D_2O): ESI Fig. S2.

GM1os preparation[15]

GM1 ganglioside (100 mg, 6.37 × 10^{-5} mol) and BSA (2.0 mg) were dissolved in 25 mM NH_4OAc, pH 5.0, 0.2% v/v Triton X-100 (9 mL). The solution was split into 450 µL aliquots, to which

EGCaseII (50 µL at 100 µM in 20 mM Na_2HPO_4, pH 7.0, 500 mM NaCl) was added. The solutions were incubated at 37 °C for 12 days, at which point TLC analysis confirmed complete reaction of the ganglioside. The solutions were combined and washed with Et_2O (2 × 10 mL), before the combined aqueous fraction was passed through a 0.45 µm syringe filter, then loaded onto a C18 solid phase extraction cartridge and eluted with H_2O. Fractions containing GM1os were combined and twice lyophilised from H_2O, yielding GM1os as a white solid (50.7 mg, 4.97×10^{-5} mol, 78% yield). The ^{1}H NMR spectrum recorded (ESI Fig. S13) is in agreement with previous reports.[37]

Immobilisation of P2-GM1os onto agarose beads

Procedure adapted from Boyer *et al*.[33] Maleimide functionalised agarose beads (Cube Biotech.) (500 µL suspension) were washed with H_2O (3 × 1 mL) and lyophilised. **P2-GM1os** (3.2 mg, 1.0×10^{-7} mol, 1.0 eq.) was dissolved in DMSO (600 µL). The solution was sparged with $N_{2(g)}$ before addition of Et_3N (25 µL, 1.8×10^{-5} mol, 180 eq.) and hexylamine (64 µL, 4.5×10^{-4} mol, 4500 eq.). The suspension was left to stir at room temperature for 16 h, then beads were isolated by centrifugation (500*g*, 1 min). The supernatant was removed and the beads were washed with H_2O (3 × 1 mL), PBS pH 7.4 (3 × 1 mL) and resuspended in 2 mM β-mercaptoethanol in PBS (500 µL). The suspension was agitated gently at room temperature for 2 h, then beads were isolated by centrifugation (500 *g*, 1 min), washed with PBS pH 7.4 (3 × 1 mL), H_2O (3 x 1 mL) and stored in 20% v/v $EtOH_{(aq)}$. UV-Vis spectra of the initial solution of **P2-GM1os** were compared to that of the supernatant after coupling (Fig. S4), with the loss of the absorbance of the trithiocarbonate unit at 309 nm demonstrating reduction of polymer end groups.

Isothermal titration calorimetry (ITC)

CTB samples were dialysed into PBS using SpectraPor dialysis tubing (MWCO 2.5 – 3 kDa, SpectrumLabs). **P2-GM1os** samples were dialysed against MilliQ H_2O, lyophilised and dissolved in the same buffer solution. The concentration of GM1os solutions in MilliQ H_2O were determined using ^{1}H NMR spectroscopic analysis[15] using EtOH as an internal standard. These solutions were then lyophilised and reconstituted in the CTB dialysis buffer prior to the titration to ensure an exact buffer match during the experiment. Concentrations of CTB stated refer to the concentrations of the subunits.

The reference cell was filled with water and the analysis cell filled with **P2-GM1os** in the case of **P2-GM1os** – CTB titrations, or CTB in the case of GM1os – CTB titrations. Both cells were allowed to reach thermal equilibrium at 25 °C, or 60 °C, before titration. Titrations typically consisted of a single 2 µL injection, followed by 29 × 8 µL injections when using the VP-ITC instrument, and single 0.5 µL injection, followed by 19 × 2 µL injections when using the ITC-200 instrument. Separate titrations of the binding partner in the syringe into buffer were used to assess the heat of dilution.

Protocol for reversible complexation of CTB

P2-GM1os beads (stored in 20% v/v $EtOH_{(aq)}$) were isolated by centrifugation (500*g*, 1 min) and resuspended in 10 µM CTB in PBS, pH 7.4 (500 µL). The tube was agitated gently at room temperature for 1 h before the beads were isolated by centrifugation (500*g*, 1 min) and the supernatant removed. **P2-GM1os** beads were washed with PBS (2 × 500 µL) at room temperature, then incubated at 60 °C in preheated PBS for 15 min. Beads were isolated by centrifugation (500 *g*, 30 s) and the elution repeated.

Protocol for purification of CTB from bacterial growth medium

Cells from a glycerol stock of *Vibrio sp60* harbouring plasmid pATA13[38] (kindly provided by Prof. Tim Hirst) were used to inoculate growth medium (100 mL, 25 g L^{-1} LB mix, 15 g L^{-1} NaCl, ampicillin 100 µgmL^{-1}). The culture was grown overnight at 30 °C with shaking at 200 rpm, then used to inoculate fresh growth medium (6 × 1 L, 25 g L^{-1} LB mix, 15 g L^{-1} NaCl, ampicillin 100 µg mL^{-1}). These cultures were incubated at 30 °C with shaking at 200 rpm until A_{600} reached 0.6 before the protein expression was induced by addition of isopropyl β-D-1-thiogalactopyranoside to a concentration of 0.5 mM. Cultures were incubated (30 °C, 200 rpm) for a further 24 h, then cells were removed by centrifugation (7500*g*, 15 min). **P2-GM1os** beads (stored in 20% v/v $EtOH_{(aq)}$) were isolated by centrifugation (500*g*, 1 min) and resuspended in the supernatant (4 × 500 µL) with a 15 min incubation time and gentle agitation at room temperature. The beads were isolated by centrifugation (500 *g*, 1 min) and the supernatant removed. **P2-GM1os** beads were washed with PBS (2 × 500 µL) at room temperature, the incubated at 60 °C in preheated PBS for 15 min. Beads were isolated by centrifugation (500*g*, 30 s) and the elution repeated.

Enzyme-linked lectin assay[20] (ELLA)

96 well high-binding black flat bottomed plates were treated with 1.3 µM GM1 ganglioside in EtOH (100 µL/well), and the solution was left to evaporate under laminar flow overnight. Wells were washed with PBS (3 × 200 µL) before treatment with 1.0% w/v bovine serum albumin (BSA) in PBS (100 µL) for 30 min at 37 °C. Wells were then washed with PBS (3 × 200 µL).

Inhibitor solutions were prepared in 0.1% w/v BSA, 0.05% Tween 20, PBS, pH 7.4 (521 µM GM1os, 100 µM **P2-GM1os**). The concentration of GM1os was determined by ^{1}H NMR spectroscopic analysis using EtOH as an internal standard.[15] A 24-step three-fold dilution series of both inhibitor solutions was performed in triplicate. Each solution was combined with a CTB-horseradish peroxidase conjugate (CTB-HRP) at 5.0 ng mL^{-1} CTB-HRP, 0.01% w/v BSA, 0.05% Tween 20, PBS, pH 7.4. These inhibitor-toxin solutions were allowed to incubate at room temperature for 2 h, then were transferred to GM1 functionalised plates (200 µL/well). The plates were left at room temperature for 30 min , then emptied and wells were washed with 0.1% w/v BSA, 0.05% Tween 20, PBS, pH 7.4 (3 × 200 µL). 5 µM H_2O_2, 5 µM Amplex red, PBS, pH 7.4 (100 µL) was added

and fluorescence was monitored over a 5 min period (λ_{ex} 531 nm, λ_{em} 595 nm) at 25 °C. The slope of each plot of fluorescence intensity against time was recorded and these values were plotted against log[inhibitor] and fitted using a standard dose-response model in Origin 8.

Human rectal biopsies

Rectal biopsies were collected from a healthy human subject after acquiring approval by the Ethics Committee of the University Medical Center Utrecht (UMCU) and after obtaining informed consent of the individual.

Generating and culturing organoids

The generation and biobanking of the intestinal organoids differed slightly from previously described protocols.[39] After washing with PBS, crypts were isolated from the biopsies, via 60-90 min incubation in 10 mM EDTA at 4 °C on a rocking platform. Crypts were collected, centrifuged at 130*g* for 5 min at 4 °C, and supernatant removed. Crypts pellet was resuspended in 50% Matrigel (Corning, diluted in culture medium), and droplets of crypts suspension were plated onto pre-warmed 24-well plates. After polymerization of the Matrigel (±15 min, 37 °C/5% CO_2), droplets were immersed in culture medium (advanced DMEM/F12 supplemented with HEPES, GlutaMAX, penicillin, streptomycin, N-2, B-27, mEGF (50 ng/ml, Life Technologies), *N*-acetylcysteine (1.25 mM), nicotinamide (10 mM), SB202190 (10 µM, Sigma), A83-01 (500 nM Tocris), prymocin (100 µg/ml, Invivogen), and 50% Wnt3a-, 20% Rspo-1-, and 10% Noggin-conditioned media). In 5-9 days, crypts grew out into full grown organoids, which were passaged via mechanical disruption of the organoids. Medium was refreshed every 2−3 days, and organoids were passaged at least two times before assays were performed.

Organoid swelling assay

CFTR function measurements in intestinal organoids was performed slightly differently than the previously described procedures.[26,39] Organoids cultured for 6-8 days were mechanically disrupted and seeded into flat-bottom 96-well plates in 50% Matrigel and incubated overnight at 37 °C, 5% CO_2. The next day, cholera toxin (Sigma C8052) was incubated together with cholera toxin inhibitors (titration) for 4 h at rt followed by staining of the organoids with 3 µM calcein AM (Invitrogen) for 15-30 min prior to organoid stimulation. Organoid swelling was monitored using the Zeiss LSM 800 confocal microscope (images were taken every 15 min during cholera/inhibitor stimulation and every 10 min during forskolin stimulation) while the organoids were kept at 37°C/5% CO_2. Organoid area increase (2D) was analyzed using Zen Blue 2.0 analysis software, and area under the curve (AUC) calculations (of the total area increase measured in 4h) were conducted with GraphPad Prism 5.0.

CTB expression and purification

Cells from a glycerol stock of *Vibrio sp60* harbouring plasmid pATA13 were used to inoculate growth medium (100 mL, 25 g L^{-1} LB mix, 15 g L^{-1} NaCl, 100 µg/mL ampicillin). The culture was grown overnight at 30 °C with shaking at 200 rpm, then used to inoculate fresh growth medium (6 x 1 L, 25 g L^{-1} LB mix, 15 g L^{-1} NaCl, ampicillin 100 µg mL^{-1}). These cultures were incubated at 30 °C with shaking at 200 rpm until A_{600} reached 0.6 before the protein expression was induced by addition of isopropyl β-D-1-thiogalactopyranoside to a concentration of 0.5 mM. Cultures were incubated (30 °C, 200 rpm) for a further 24 h, then cells were removed by centrifugation (7500*g*, 15 min). The combined supernatant was treated with ammonium sulphate (550 g L^{-1}) and left to stir at 5 °C overnight. Crude protein was isolated by centrifugation (17,000*g*, 25 min) and redissolved in in 100 mM NaH_2PO_4, pH 7.0, 500 mM NaCl (60 mL). Insoluble material was removed by centrifugation (5000*g*, 10 min) before the solution was passed through a 0.22 µm filter then loaded onto a lactose-sepharose 6B column and eluted with 300 mM lactose, 100 mM NaH_2PO_4, pH 7.0, 500 mM NaCl. CTB was dialysed against PBS, pH 7.4, freeze-dried and stored at -80 °C.

Expression of EGCaseII[24]

A synthetic gene for endoglycosylceramidase from *Rhodococcus sp. M-777*) bearing an N-terminal His-tag and codon-optimised for expression in *E. coli* in a pET28a backbone was purchased from Genscript (Piscataway, USA). Cells from glycerol stock (*E. coli* BL21 (DE3) gold) were used to inoculate TYP broth (100 mL, 16 g L^{-1} tryptone, 16 g L^{-1} yeast, 5 g L^{-1} NaCl, 2.5 g L^{-1} K_2HPO_4, 50 µg mL^{-1} kanamycin) and the culture was grown at 37 °C with shaking at 200 rpm overnight. The temperature was decreased to 20 °C before protein expression was induced by addition of isopropyl β-D-1-thiogalactopyranoside to a final concentration of 0.1 mM. The culture was incubated at 20 °C with shaking at 200 rpm for 7.5 h before cells were isolated by centrifugation (5000*g*, 10 min) and cell pellets stored at -20 °C overnight. Cell pellets were resuspended in BugBuster (5 mL) and left at room temperature for 30 min before cell debris was removed by centrifugation (5000*g*, 15 min) and supernatant was applied to a Ni-NTA column which had been pre-equilibrated with 20 mM Na_2HPO_4, pH 7.0, 0.5 M NaCl. The flow-through was passed through the column again, before the column was washed with 20 mM Na_2HPO_4, pH 7.0, 0.5 M NaCl (20 mL), then eluted with a stepwise imidazole gradient (10 mL aliquots: 50, 100, 200 300, 400, 500 mM imidazole) in the same buffer. Elutions at 100 mM and 200 mM imidazole were combined and dialysed against 20 mM Na_2HPO_4, pH 7.0, 0.5 M NaCl. ECGaseII was concentrated to 100 µM, divided into 50 µL aliquots and stored at -80 °C.

Conflicts of interest

There are no conflicts to declare.

Acknowledgements

CSM wishes to thank EPSRC and the University of Leeds for the award of a Doctoral Prize Fellowship which enabled this work. WBT acknowledges the support of BBSRC (BB/M005666/1). The

authors thank Dr David A. Fulton, Newcastle University, UK, for access to gel permeation chromatography equipment.

Notes and references

1. L.-G. Milroy, T. N. Grossmann, S. Hennig, L. Brunsveld and C. Ottmann, *Chem. Rev.*, 2014, **114**, 4695-4748.
2. H. Yin and A. D. Hamilton, *Angew. Chem. Int. Ed.*, 2005, **44**, 4130-4163.
3. V. Azzarito, K. Long, N. S. Murphy and A. J. Wilson, *Nature Chem.*, 2013, **5**, 161.
4. J. D. Badjić, A. Nelson, S. J. Cantrill, W. B. Turnbull and J. F. Stoddart, *Acc. Chem. Res.*, 2005, **38**, 723-732.
5. M. V. Walter and M. Malkoch, *Chem. Soc. Rev.*, 2012, **41**, 4593-4609.
6. C. S. Mahon, C. J. McGurk, S. M. D. Watson, M. A. Fascione, C. Sakonsinsiri, W. B. Turnbull and D. A. Fulton, *Angew. Chem. Int. Ed.*, 2017, **56**, 12913-12918.
7. C. S. Mahon, M. A. Fascione, C. Sakonsinsiri, T. E. McAllister, W. B. Turnbull and D. A. Fulton, *Org. Biomol. Chem.*, 2015, **13**, 2756-2761.
8. Y. Gou, J. Geng, S.-J. Richards, J. Burns, C. Remzi Becer and D. M. Haddleton, *J. Polym. Sci. A Polym. Chem.*, 2013, **51**, 2588-2597.
9. G. Kocak, C. Tuncer and V. Butun, *Polym. Chem.*, 2017, **8**, 144-176.
10. S. Won, S.-J. Richards, M. Walker and M. I. Gibson, *Nanoscale Horiz.*, 2017, **2**, 106-109.
11. E. J. Sayers, J. P. Magnusson, P. R. Moody, F. Mastrotto, C. Conte, C. Brazzale, P. Borri, P. Caliceti, P. Watson, G. Mantovani, J. Aylott, S. Salmaso, A. T. Jones and C. Alexander, *Bioconjugate Chem.*, 2018, **29**, 1030-1046.
12. K. Yoshimatsu, B. K. Lesel, Y. Yonamine, J. M. Beierle, Y. Hoshino and K. J. Shea, *Angew. Chem. Int. Ed.*, 2012, **51**, 2405-2408.
13. A. Bratek-Skicki, V. Cristaudo, J. Savocco, S. Nootens, P. Morsomme, A. Delcorte and C. Dupont-Gillain, *Biomacromolecules*, 2019, DOI: 10.1021/acs.biomac.8b01353.
14. D. Vanden Broeck, C. Horvath and M. J. S. De Wolf, *Int. J. Biochem. Cell Biol.*, 2007, **39**, 1771-1775.
15. W. B. Turnbull, B. L. Precious and S. W. Homans, *J. Am. Chem. Soc.*, 2004, **126**, 1047-1054.
16. A. Bernardi, J. Jimenez-Barbero, A. Casnati, C. De Castro, T. Darbre, F. Fieschi, J. Finne, H. Funken, K.-E. Jaeger, M. Lahmann, T. K. Lindhorst, M. Marradi, P. Messner, A. Molinaro, P. V. Murphy, C. Nativi, S. Oscarson, S. Penades, F. Peri, R. J. Pieters, O. Renaudet, J.-L. Reymond, B. Richichi, J. Rojo, F. Sansone, C. Schaffer, W. B. Turnbull, T. Velasco-Torrijos, S. Vidal, S. Vincent, T. Wennekes, H. Zuilhof and A. Imberty, *Chem. Soc. Rev.*, 2013, **42**, 4709-4727.
17. S. Cecioni, A. Imberty and S. Vidal, *Chem. Rev.*, 2015, **115**, 525-561.
18. A. V. Pukin, H. M. Branderhorst, C. Sisu, C. A. G. M. Weijers, M. Gilbert, R. M. J. Liskamp, G. M. Visser, H. Zuilhof and R. J. Pieters, *ChemBioChem*, 2007, **8**, 1500-1503.
19. C. L. Schengrund and N. J. Ringler, *J. Biol. Chem.*, 1989, **264**, 13233-13237.
20. T. R. Branson, T. E. McAllister, J. Garcia-Hartjes, M. A. Fascione, J. F. Ross, S. L. Warriner, T. Wennekes, H. Zuilhof and W. B. Turnbull, *Angew. Chem. Int. Ed.*, 2014, **53**, 8323-8327.
21. E. S. Gil and S. M. Hudson, *Prog. Polym. Sci.*, 2004, **29**, 1173-1222.
22. Y. Chen, N. Ballard, O. D. Coleman, I. J. Hands-Portman and S. A. F. Bon, *J. Polym. Sci. A Polym. Chem.*, 2014, **52**, 1745-1754.
23. M.-r. Lee and I. Shin, *Org. Lett.*, 2005, **7**, 4269-4272.
24. M. D. Vaughan, K. Johnson, S. DeFrees, X. Tang, R. A. J. Warren and S. G. Withers, *J. Am. Chem. Soc.*, 2006, **128**, 6300-6301.
25. M. Ito, *Trends Glycosci. Glycotechnol.*, 1990, **2**, 399-402.
26. V. Kumar and W. B. Turnbull, *Beilstein J. Org. Chem.*, 2018, **14**, 484-498.
27. H. Zuilhof, *Acc. Chem. Res.*, 2016, **49**, 274-285.
28. D. D. Zomer-van Ommen, A. V. Pukin, O. Fu, L. H. C. Quarles van Ufford, H. M. Janssens, J. M. Beekman and R. J. Pieters, *J. Med. Chem.*, 2016, **59**, 6968-6972.
29. M. Garland, S. Loscher and M. Bogyo, *Chem. Rev.*, 2017, **117**, 4422-4461.
30. C. Sisu, A. J. Baron, H. M. Branderhorst, S. D. Connell, C. A. G. M. Weijers, R. de Vries, E. D. Hayes, A. V. Pukin, M. Gilbert, R. J. Pieters, H. Zuilhof, G. M. Visser and W. B. Turnbull, *ChemBioChem*, 2009, **10**, 329-337.
31. B. Goins and E. Freire, *Biochemistry*, 1988, **27**, 2046-2052.
32. E. A. Merritt, T. K. Sixma, K. H. Kalk, B. A. M. van Zanten and W. G. J. Hol, *Mol. Microbiol.*, 1994, **13**, 745-753.
33. X. Huang, C. Boyer, T. P. Davis and V. Bulmus, *Polym. Chem.*, 2011, **2**, 1505-1512.
34. M. Alam, N. A. Hasan, M. Sultana, G. B. Nair, A. Sadique, A. S. G. Faruque, H. P. Endtz, R. B. Sack, A. Huq, R. R. Colwell, H. Izumiya, M. Morita, H. Watanabe and A. Cravioto, *J. Clin. Microbiol.*, 2010, **48**, 3918-3922.
35. A. K. Pearce, B. E. Rolfe, P. J. Russell, B. W. C. Tse, A. K. Whittaker, A. V. Fuchs and K. J. Thurecht, *Polym. Chem.*, 2014, **5**, 6932-6942.
36. J. T. Lai, D. Filla and R. Shea, *Macromolecules*, 2002, **35**, 6754-6756.
37. S. Sabesan, K. Bock and R. U. Lemieux, *Can. J. Chem.*, 1984, **62**, 1034-1045.
38. A. T. Aman, S. Fraser, E. A. Merritt, C. Rodigherio, M. Kenny, M. Ahn, W. G. J. Hol, N. A. Williams, W. I. Lencer and T. R. Hirst, *Proc. Natl Acad. Sci. USA*, 2001, **98**, 8536-8541.
39. J. F. Dekkers, C. L. Wiegerinck, H. R. de Jonge, I. Bronsveld, H. M. Janssens, K. M. de Winter-de Groot, A. M. Brandsma, N. W. M. de Jong, M. J. C. Bijvelds, B. J. Scholte, E. E. S. Nieuwenhuis, S. van den Brink, H. Clevers, C. K. van der Ent, S. Middendorp and J. M. Beekman, *Nat. Med.*, 2013, **19**, 939-945.